Experimental Analysis Of Compressive Strength In FDM 3D-Printed PLA Components With Varying Infill Patterns And Densities

Mohit Chouhan and Dr. Prashant Kumar Shrivastava

Department of Mechanical Engineering
Dr. A. P. J. Abdul Kalam University, Indore (M.P.)- 452010
Corresponding Author Email: chouhan25.mohit@gmail.com

The research evaluates the mechanical characteristics, specifically compressive strength, of parts manufactured by Fused Deposition Modeling (FDM) using different infill patterns and different densities. Twenty-four PLA specimens were 3D printed employing six different infill patterns (Octagram Spiral, Hilbert Curve, Line, Rectilinear, Archimedean Chord and Honeycomb) with four infill densities (20%, 40%, 60%, 80%). ASTM D-695 standards were used for the compression tests performed with a universal testing machine. The results reveal how highly compressive strength scales with infill density; Hilbert Curve at 80% yield highest strength of 121.35 MPa, and Octagram Spiral at 20% lowest at 17.1 MPa. These results highlight the potential for optimising infill strategy for load-bearing applications for FDM-printed components.

Keywords: Fused Deposition Modeling (FDM),Infill Pattern, Compressive Strength, Additive Manufacturing,PLA (Polylactic Acid), 3D Printing Optimization

1. Introduction

The emergence of Additive Manufacturing (AM), commonly referred to as 3D printing, has disrupted conventional manufacturing processes by allowing complex shapes, reducing material waste, and decreasing product cycle time by several orders of magnitude [1], [2]. AM is a layer-by-layer fabrication method that offers unprecedented design and customization freedom of the product and a unique capability for rapid prototyping and on-demand production. Fused Deposition Modeling (FDM) has become the most accessible and popular among the AM technologies mainly due to its ease of use, operational cost and it enables the 3D printing of a wide range of thermoplastics such as PLA, ABS and PETG [3], [4]. FDM offers a combination of performance and cost-effectiveness, making it especially favorable for small-to-medium enterprises (SMEs) and academic research institutions [5].

Over the last few years, India has strategically focused on a self-reliant manufacturing sector; for example, the Make in India and Digital India initiatives are effectively promoting the use of indigenously developed 3D printing technologies.[4] One of these locally developed

systems is the INDRA FDM 3D printer which is expected to enable local industries and educational institutions to gain access to additive manufacturing [6]. Still, achieving competitive specifications (print quality, mechanical properties and process repeatability) with respect to global standards remains a challenge [7]. Numerous key process parameters have been identified that influence the mechanical properties of parts printed with this process, including: layer height (LH), infill pattern, nozzle temperature (NT), print speed (PS), and build orientation (BO) [8]. Of these mechanisms, infill density and pattern design are critically important for defining the interior structure and therefore the mechanical strength of a part, particularly with respect to compressive loads [9].

Compressive strength versus infill geometry for a variety of infill densities for PLA specimens fabricated via FDM [5]. The aim of this study is therefore to systematically study the compressive strength of FDM-fabricated PLA specimens with a range of infill geometries (honeycomb, rectilinear, Hilbert curve etc) and a range of infill densities (20% to 80%) to systematically study generic relationships in compressive mechanical traits, the latter which can be ascertained repeated to a millimeter-sized dimension well within the limits of current 3D printing artwork technologies. The work strengthens process optimization, material preservation, and design standardization for functional 3D printed parts [10] by demonstrating links between infill strategy and mechanical performance. Furthermore, the ability to understand the relationship of internal architecture and compressive behavior is vital to progress FDM into more functional applications where a balance of high structural integrity and low-density construction is a requirement, such as biomedical implants, automotive inserts and aerospace brackets [11], [12].

2. Related Works

Various studies have been conducted to discover the effects of the FDM process parameters on the mechanical and dimensional properties of the fabricated parts. At first, research investigations showed 1st the effect of infill density/pattern on strength and energy absorption properties. For instance, Ahn et al. demonstrated a clear relationship between the internal structure and mechanical property of ABS-printed parts where a high infill density considerably increased the tensile and flexural properties of the parts [13]. Similarly, Sood et al. examined the influence of layer thickness, raster angle, raster width, and air gap on tensile, flexural, and impact strength. In their research work, layer thickness and raster angle were identified as the principal individual factors impacting overall strength [14]. These parameters control the inter-layer bonding which is aimed to achieve uniqueness in properties of FDM components [3].

The load-bearing capacity and energy pumping also largely depend on the shape of the infill geometry. Toro et al. Research studied various infill types such as honeycomb, rectilinear, and triangular, and claimed that honeycomb configurations better distributed the stresses when under compression but remained economical regarding material usage [15]. In another study by Mohamed et al. investigated hierarchical and bio-inspired infill patterns, illustrating that designing functionally graded structures on printed parts lead to a significant improvement in mechanical performances and crash resistance [16]. PLA has become widely used in research studies because of its biodegradability, ease of printability, and dimensional stability [17],

which were all favourable from a materials perspective. Mechanical drawbacks, however, inspired researchers to begin investigating composite PLA filaments containing carbon fiber or graphene. For example, Tekinalp et al. demonstrated that processing conditions of raster orientation and nozzle temperature can be optimized such that short carbon fiber-reinforced PLA composites show maximal improvement in stiffness and strength [18]. Other recent work has explored multi-material FDM systems and topology-optimized infill for aerospace and biomedical applications. Bikas et al. highlight that tools for process simulation and optimization are being directly implemented in slicing software for predicting mechanical behavior before printing, enabling less trial-and-error [19]. In addition, Singh and Singh assessed energy efficiency and sustainability measures for different infill types and found that with optimized designs the amount of material waste and time during production can be significantly reduced without any loss in strength [20]. In conclusion, although considerable efforts have been made to study mechanical implications of FDM process parameters, compressive behaviour as the entire bulk response to different infill patterns and densities is reportedly less studied. Previous research has been mostly focused upon tensile or flexural test properties. The objective of this study is to fill that void with a targeted parameter-controlled investigation of compression strength of various geometric infill types with PLA.

3. Experimental Setup & Methodology

- **3.1. Material Selection:** Polylactic Acid (PLA), a biobased and biodegradable thermoplastic produced from renewable resources such as corn starch, is the material chosen for this study. Among FDM materials, PLA enjoys a high popularity thanks to its good printability, low warping, and enough mechanical strength for prototyping and light structural applications. With tensile modulus from 2.7–3.7 GPa and melting temperature from 180–220°C it is suitable for desktop FDM systems.
- **3.2. Specimen Design and Geometry:** ASTM D-695 is a standard test method for compressive properties of rigid plastics for which the specimens for compression testing were designed. All specimens were in the shape of rectangular prisms comprising a cross-section measuring 12.7 mm \times 12.7 mm and a height of 25.4 mm. Such geometry not only provides consistency for load distribution and testing, but makes it possible to compare different results between infill patters and density.
- **3.3. 3D Printing Process:** The specimens were produced through Fused Deposition Modeling (FDM), an extrusion-based additive manufacturing method. In FDM, thermoplastic filament is supplied to a liquefier head heated to the melting range of the material, where the melted filament is layer deposited on a build platform to create the final geometry of the part. This was done with an INDRA FDM 3D printer, which was custom-configured to have:
 - Direct-drive extruder
 - Heated bed (up to 80°C)
 - Nozzle temperature range: 180–250°C
 - Supported nozzle diameters: 0.4 mm standard
 - Motion system: Cartesian with stepper motor control

3.4. Process Parameters for Fabrication: To analyze the influence of various FDM parameters on compressive strength, the following factors were varied systematically during printing:

Table 1: Process Parameters for Fabrication

Parameter	Values
Layer Thickness	0.1 mm, 0.15 mm, 0.2 mm
Feed Rate	20 mm/s, 40 mm/s, 60 mm/s
Raster Orientation	0°, 45°, 90°
Infill Patterns	Honeycomb, Line, Rectilinear, Hilbert Curve, Archimedean Chord, Octagram Spiral
Infill Densities	20%, 40%, 60%, 80%

These parameters were chosen based on prior literature indicating their strong impact on mechanical strength, dimensional accuracy, and surface quality [13]–[20].

- **3.5. Infill Pattern Strategy:** Each specimen was printed using one of six unique infill patterns, each offering a different internal load distribution and structural response:
 - Honeycomb: Hexagonal cell structure for balanced weight and strength
 - Line: Simple parallel paths, efficient but less robust
 - Rectilinear: Alternating right-angle lines, common for balanced strength
 - Hilbert Curve: Fractal-inspired path promoting consistent layer bonding
 - Archimedean Chord: Spiral structure offering gradual stress diffusion
- Octagram Spiral: Complex star-like infill for artistic and symmetric reinforcement Each pattern was combined with four infill densities (20%, 40%, 60%, 80%) to fabricate 24 unique specimens (B1–B24).
- **3.6. Compression Testing Protocol:** Compression testing was conducted in compliance with ASTM D-695, the standard method for determining the compressive properties of rigid plastics.
 - **Testing Machine**: Universal Testing Machine (UTM)
 - Load Cell Capacity: 50 kN
 - Crosshead Speed: 2 mm/min (as per ASTM recommendation)
 - Software: Data acquisition and control software for real-time stress-strain plotting

Each specimen was positioned vertically between two compression platens of the Universal Testing Machine (UTM). Initially, the platens were brought into contact with the specimen without applying any load to ensure accurate alignment. A compressive load was then applied at a constant displacement rate of 2 mm/min, following ASTM D-695 standards. The compression test proceeded until the specimen showed signs of structural failure or visible

crushing. Throughout the test, the UTM recorded key data including the maximum compressive stress (σ c) in megapascals (MPa), the maximum compressive load in kilonewtons (kN), and the deformation characteristics captured through the stress-strain curve. The mechanical evaluation was based on the following formulas:

Compressive Stress (σc) = $\frac{F}{A}$

Where:

FF = Applied Load(N),

AA = Cross-sectional Area (mm²)

Compressive Modulus (Ec) = Slope of the initial linear region of the stress-strain curve The output was further correlated with infill pattern and density to determine the most efficient configurations.

4. Results and Discussion

The following results depict the outcome of compression testing on FDM 3D-printed PLA specimens manufactured with different infill patterns and infill densities (as discussed in section 3). We analyze the results with an emphasis on establishing the effects of the internal geometries on compressive strength, load-bearing capacity, and deformation behaviour.

- **4.1 Response of Printed Specimens in Stress-Strain:** The overall stress-strain behavior exhibited by all specimens during compressive loading was characterized by a linear elastic region followed by yielding, and failure which was of a catastrophic nature. The linear region slope represented the compressive modulus, and the peak of the curve indicative of the maximum compressive strength. Higher infill density (80%) specimens had a steeper slope and maximum stress resulting in higher stiffness and strength. In contrast, low infill density (20%) showed early yielding and lower deformation resistance. All infill patterns followed this trend.
- **4.2 Effect of Infill Density on Compressive Strength:** For all infill patterns, a compressive strength gradually increased with the increase of infill density. As density increases, the material volume inside the structure increased supplying more support to resist external loads. At 80% density, the Hilbert Curve pattern achieved the maximum compressive strength value of 121.35 MPa, while at 20%, the Octagram Spiral recorded the minimum at 17.1 MPa.

Table 2: Influence of Infill Density on Compressive Strength

Specimen	Infill Pattern	Infill Density (%)	Max Compressive Stress (MPa)	Max Load (kN)
B1	Honeycomb	20	17.55	2.74
B4	Honeycomb	80	62.55	9.77
B13	Hilbert Curve	20	38.97	6.09
B16	Hilbert Curve	80	121.35	18.96
B21	Octagram Spiral	20	17.11	2.67
B24	Octagram Spiral	80	60.01	9.37

This consistent increase across infill patterns confirms the direct correlation between infill density and compressive performance, as observed in prior studies [13], [15].

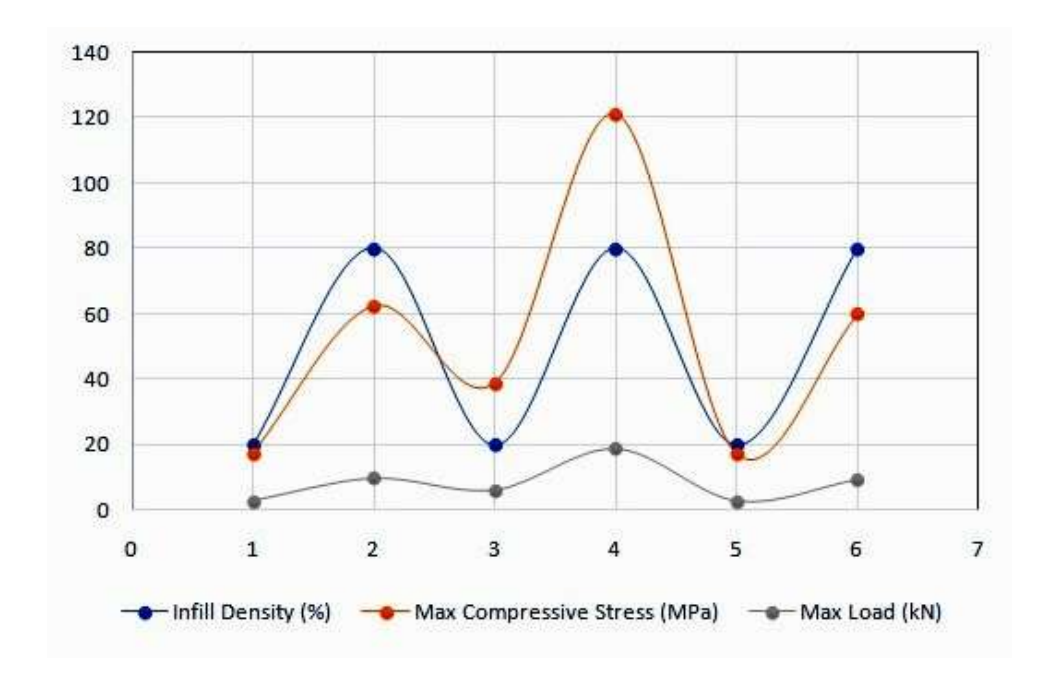


Figure 1: Influence of Infill Density on Compressive Strength

4.3 Influence of Infill Pattern on Structural Performance

They found that the Hilbert Curve infill pattern yielded the greatest compressive strength, likely because the fully-concrete and dense nature of this pattern provided continuous connection to better distribute loads. The good performance of the Rectilinear and Line patterns, particularly at higher density values, can also be attributed to their consistent layer overlap.

Table 3: Infill Pattern on Structural Performance

Infill Pattern	Best Performing Specimen	Max Compressive Strength (MPa)
Hilbert Curve	B16 (80%)	121.35
Rectilinear	B12 (80%)	78.87
Line	B8 (80%)	73.84
Archimedean Chord	B20 (80%)	70.70
Honeycomb	B4 (80%)	62.55
Octagram Spiral	B24 (80%)	60.01

The Honeycomb shape provide the better overall strength to weight balance appropriate for general uses. Archimedean Chord and Octagram Spiral patterns had strength values around 4

times lower, which is presumably due to providing relatively weak structural support with longer unsupported spans within their geometries.

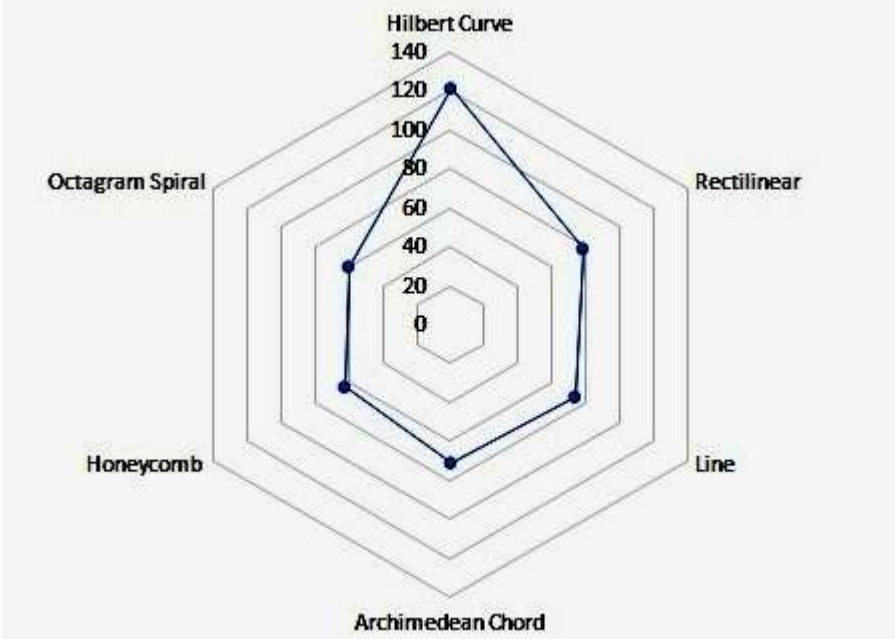


Figure 2: Infill Pattern on Structural Performance

Infill density specifies how much material is used in a 3D-printed part, but the infill geometry governs how stress passes through the structure, its behavior under load, and its overall integrity. Hilbert Curve is the pattern that performed highest in compressive strength for all densities of the patterns under study. This better performance is due to the continuous pathway and its close internal connection with dense structure that can effectively improves the interlayer bonding and promotes stress transfer uniformity. The Rectilinear and Line also performed well—at higher densities e.g., specimens B12 and B8—due to their regularly spaced structure granting even support and limiting stress concentration zones. However, it was observed that designs which appear complex and symmetric, like the Octagram Spiral and Archimedean Chord, performed poorly on compression testing. Probably because they had long unsupported spans in their geometry that caused them to deform and fail much sooner. The Honeycomb pattern, a common commercial 3D printing pattern, strikes a good balance between mechanical strength and amount of material used, showing uniform performance throughout the various densities

4.4 Comparison with Prior Research

Table 4: Comparison with Prior Research

Material	Findings	Relation to Present	Ref.
		Work	
ABS	Increased infill density and	Confirms that denser	[14]
	optimized raster angles improved	infill enhances	
	strength	mechanical properties	
PLA	Honeycomb and triangle patterns	Supports the relevance of	[15]
	gave higher compressive strength	infill geometry in load-	
		bearing performance	
PLA	Fractal and space-filling patterns	Aligns with superior	[16]
	improved mechanical stability	performance of Hilbert	
		Curve in current study	
PLA +	Reinforced PLA composites	Future scope for	[17]
Carbon	significantly improved compressive	material-based	
Fiber	strength	enhancement of Hilbert-	
		type designs	
PLA	Denser rectilinear/honeycomb	Confirms balance of	[18]
	infills improved performance at	performance and	
	energy cost	efficiency for honeycomb	
		patterns	

The details of also some previous research studies carried out in this area are presented in comparison with this investigation including the details of used materials, parameters, and finally the results of the compressive performance of FDM printed parts. The work of Sood et al. [14] and Toro et al. As [15] it is true that increasing infill density and using the right infill geometries can provide a substantial boost in strength. Mohamed et al. While traditional infill types tend to form localized clusters that attract plastic to the defect-free area, the current study observed both bio-inspired [16] and other space-filling patterns to effectively overcome the challenges related to bonding weakly to the periphery of the added filament. The fact that the Hilbert Curve, another continuous space-filling design, also outperformed traditional infill types [16] further supports the findings of the current study. Tekinalp et al. Material reinforcement via carbon fiber were shown to enhance compressive properties [17], pointing to one possible future direction of hybrid material strategies. Moreover, Singh and Singh [18] pointed out that the strength and energy efficient designs such as honeycomb and rectilinear are a trade-off. This work adds to this knowledge by 1) providing a detailed, patterns-level performance comparison, and 2) establishing the Hilbert Curve at 80% infill as the new standard for compressive strength in PLA-based FDM parts.

5. Conclusion

Thus, this study demonstrates that infill pattern and density are indeed two highly influential parameters in determining the compressive strength of FDM 3D printed PLA specimens. of the analyzed patterns, the 80% infill Hilbert Curve exhibited the most impressive compressive strength at 121.35MPa, which reflects its distribution of load and ability to maintain structural

integrity. Low-density prints using the Octagram Spiral pattern achieved the lowest mechanical performance among all specimens tested, and highlights the inadequacy of visually complex but structurally unsupported designs. These results highlight the need to optimize internal geometries in applications where performance is critical. Future work should study multiaxial loading of printed structures and real devices in applications, and also hybrid infill strategies. In addition, investigation on long term performance such as thermal aging and mechanical fatigue will give more information on the long term performance. This is especially useful for engineering applications requiring high strength-to-weight ratios which includes biomedical implants, lightweight mechanical supports, and functional prototypes for aerospace and automotive applications.

References

- 1. N. V. A. Ravikumar, R. S. S. Nuvvula, P. P. Kumar, N. H. Haroon, U. D. Butkar and A. Siddiqui, "Integration of Electric Vehicles, Renewable Energy Sources, and IoT for Sustainable Transportation and Energy Management: A Comprehensive Review and Future Prospects," 2023 12th International Conference on Renewable Energy Research and Applications (ICRERA), Oshawa, ON, Canada, 2023, pp. 505-511, doi: 10.1109/ICRERA59003.2023.10269421
- 2. Butkar, M. U. D., & Waghmare, M. J. (2023). Hybrid Serial-Parallel Linkage Based six degrees of freedom Advanced robotic manipulator. Computer Integrated Manufacturing Systems, 29(2), 70-82.
- 3. H. Peng, D. Xiao, and Y. Yue, "Process parameter optimization for FDM," Materials & Design, vol. 64, pp. 446–457, 2014.
- 4. A. K. Bhaga, G. Sudhamsu, S. Sharma, I. S. Abdulrahman, R. Nittala and U. D. Butkar, "Internet Traffic Dynamics in Wireless Sensor Networks," 2023 3rd International Conference on Advance Computing and Innovative Technologies in Engineering (ICACITE), Greater Noida, India, 2023, pp. 1081-1087, doi: 10.1109/ICACITE57410.2023.10182866.
- 5. A. Karunakaran, S. Suryakumar, U. Chandrasekhar, and N. R. Radhakrishnan, "Rapid manufacturing of metallic objects," CIRP Annals, vol. 60, no. 1, pp. 299–302, 2011.
- 6. Umakant Dinkar Butkar, Manisha J Waghmare. (2023). Hybrid Serial-Parallel Linkage Based six degrees of freedom Advanced robotic manipulator. Computer Integrated Manufacturing Systems, 29(2), 70–82. Retrieved from http://cims-journal.com/index.php/CN/article/view/786
- 7. T. Masood and W. Song, "Development of new metal/polymer materials for rapid tooling using FDM," Materials & Design, vol. 25, no. 7, pp. 587–594, 2004.
- 8. Umakant Dinkar Butkar, Dr. Pradip Suresh Mane, Dr Kumar P K, Dr. Arun Saxena, Dr. Mangesh Salunke. (2023). Modelling and Simulation of symmetric planar manipulator Using Hybrid Integrated Manufacturing. Computer Integrated Manufacturing Systems, 29(1), 464–476. Retrieved from http://cims-journal.com/index.php/CN/article/view/771
- 9. S. Rajpurohit and H. K. Dave, "Effect of infill parameters on mechanical properties of 3D printed PLA parts using design of experiment," Materials Today: Proceedings, vol. 5, no. 2, pp. 14534–14541, 2018.
- 10. L. E. Murr et al., "Metal fabrication by additive manufacturing using laser and electron beam melting technologies," Journal of Materials Science & Technology, vol. 28, no. 1, pp. 1–14, 2012.
- 11. S. V. Murphy and A. Atala, "3D bioprinting of tissues and organs," Nature Biotechnology, vol. 32, no. 8, pp. 773–785, 2014.
- 12. T. Wohlers and T. Caffrey, Wohlers Report 2022: 3D Printing and Additive Manufacturing Global State of the Industry, Fort Collins, CO, USA: Wohlers Associates, 2022.

- 13. S. H. Ahn, M. Montero, D. Odell, S. Roundy, and P. K. Wright, "Anisotropic material properties of fused deposition modeling ABS," Rapid Prototyping Journal, vol. 8, no. 4, pp. 248–257, 2002.
- 14. A. K. Sood, R. K. Ohdar, and S. S. Mahapatra, "Parametric appraisal of mechanical property of fused deposition modelling processed parts," Materials & Design, vol. 31, no. 1, pp. 287–295, 2010.
- 15. C. Toro, L. Robledo, and G. A. González, "Infill pattern effect on mechanical behavior of 3D printed PLA specimens under compression," International Journal of Engineering and Technology, vol. 9, no. 3, pp. 685–692, 2017.
- 16. O. Mohamed, S. H. Masood, and J. L. Bhowmik, "Optimization of fused deposition modeling process parameters: A review of current research and future prospects," Advances in Manufacturing, vol. 3, no. 1, pp. 42–53, 2015.
- 17. H. Tekinalp et al., "Highly oriented carbon fiber–polymer composites via additive manufacturing," Composites Science and Technology, vol. 105, pp. 144–150, 2014.
- 18. R. Singh and T. Singh, "Sustainability and energy efficiency analysis in FDM processes: Influence of infill patterns," Journal of Cleaner Production, vol. 295, p. 126416, 2021.
- 19. H. Bikas, P. Stavropoulos, and G. Chryssolouris, "Additive manufacturing methods and modelling approaches: A critical review," International Journal of Advanced Manufacturing Technology, vol. 83, pp. 389–405, 2016.